Development of a calibration chamber system for testing at high confining pressures

Matthew Haynes[1], *David* Reid[2], *Riccardo* Fanni[1,2#], and *Kyle* Smith[1*]

[1]*WSP Australia, Mine Waste, Perth, Australia, matthew.haynes@wsp.com*
[2]*University of Western Australia, Department of Civil, Environmental, and Mining Engineering, Perth, david.reid@uwa.edu.au*
[#]*riccardo.fanni@wsp.com*
**kyle.smith2@wsp.com*

ABSTRACT

Cone penetration testing with pore pressure measurement (CPTu) represents a state of practice tool to assess the in situ state parameter, strength, and liquefaction susceptibility of sandy soils and mine tailings. Many techniques for the interpretation of CPTu data are based on the results of calibration chamber test programs on sand and, more recently, mine tailings. While these efforts have led to the current methods to interpret CPTu data, two factors relevant to CPTu interpretation require consideration: (i) the available calibration chamber data is dominated by tests with consolidated mean effective stresses < 200 kPa; and (ii) tailings storage facilities are being constructed to heights such that in situ effective stresses are far higher than those of the available calibration chamber test database. While much of CPTu interpretation is carried out in a dimensionless framework, there is evidence that existing relationships between stress-normalised tip resistance and state parameter are dependent on effective stress. This stress-dependence has been attributed to a variation in shear rigidity with effective stress, which is not accounted for in many interpretation techniques. However, at high stresses, other factors such as the curvature of the critical state line in an e-log(p') plane may contribute. To assess CPTu of sands at high stresses, a novel small-scale calibration chamber employing a miniature cone capable of testing soils consolidated to a mean effective stress up to 2,000 kPa is outlined. Test results are presented for tests carried out over a range of mean effective stresses up to 1,000 kPa.

Keywords: CPTu; calibration chamber; high stress; tailings.

1. Introduction

Characterisation of tailings is crucial for design analyses of tailings storage facilities (TSFs). A combination of in situ and laboratory tests are used to estimate the strength of tailings. However, the in situ strength of low plasticity silt and sand tailings can be difficult to infer through laboratory testing due to significant sampling disturbance. Therefore, in situ tests such as the cone penetration test with pore pressure measurement (CPTu) are required to estimate the state parameter (Ψ) of the tailings.

Current state of practice methods to estimate Ψ from normalised CPTu tip resistance (Q) have been developed by Been, Crooks, and Jefferies (1988) and Been and Jefferies (1992) based on a database of calibration chamber testing. Tip resistance was normalised by Been and Jefferies according to Eq. (1), where Q_p is the tip resistance (q_t) normalised by mean total stress (p) and mean effective stress (p'). Further, Eq. (2) normalises Q_p by pore pressure ratio (B_q) and presents the relationship with Ψ and coefficients k and m. Finally, Shuttle and Cunning (2007) introduced Eq. (3), which is the form used in this paper.

$$Q_\mathrm{p} = \frac{q_\mathrm{t} - p}{p'} \tag{1}$$

$$q^* = \frac{Q_\mathrm{p}}{1 - B_\mathrm{q}} = k\mathrm{e}^{-m\Psi} \tag{2}$$

$$Q_\mathrm{p}\left(1 - B_\mathrm{q}\right) + 1 = k\mathrm{e}^{-m\Psi} \tag{3}$$

Shuttle and Jefferies (2016) introduced the cavity expansion model, CPTwidget, to provide an alternative to undertaking physical calibration chamber testing. The results of CPTwidget were scaled using a cone factor (C_q) to match calibration chamber tests from the updated database used by Jefferies and Been (2015). CPTwidget allows for calibration of Q vs Ψ over a range of shear rigidity (I_r) values to capture the influence of I_r variation with effective stress. Variation of I_r is the only stress dependent relationship in CPTwidget for drained simulations. However, materials with a curved critical state line (CSL), where λ_e (ln of λ) changes with stress, may also have the λ_e input varied with stress, although guidance for this is not provided by the authors.

The calibration chamber database used by Jefferies and Been (2015) has been limited to a maximum p' of 457 kPa, with a mean and median of 109 and 75 kPa, respectively. This database of tests was used by Shuttle and Jefferies (2016) to develop state of practice techniques for calibration of Q vs Ψ. Tests on Ticino sand at stresses between p' = 27 to 451 kPa show a clear stress-level bias which Jefferies and Been have attributed to the variation of I_r with stress.

This paper presents a comparison of small-scale calibration chamber testing using a miniature CPTu cone at low and high effective stress. A sand with appreciable curvature of the CSL at high stress was tested. Comparison to CPTwidget simulations allows for an assessment of the stress dependence of CPTwidget by varying I_r and λ_c.

2. Calibration chamber

2.1. Equipment

A small-scale calibration chamber was created based on a triaxial testing apparatus, similar to the design presented by Ayala, Fourie, and Reid (2020) and Damavandi-Monfared and Sadrekarimi (2015). The calibration chamber applies stress isotropically using cell pressure applied to the membrane and top cap. The steel bottom cap applies a fixed base restraint. Therefore, the boundary conditions are classified as BC4 (Been et al. 1986). The following equipment was used:

- 488 × 222 mm (internal height × diameter) triaxial cell with coupling to seal against the shaft of the CPTu apparatus.
- 2 × pressure/volume controllers to apply the cell and back (specimen pore) pressure.
- 200 mm diameter top and bottom caps. The top cap includes a sealed opening for the shaft of the CPTu apparatus.
- 2 × 200 mm sintered-bronze porous stones for the top and bottom of the specimen. The top porous stone includes an opening for the CPTu cone.
- 430 × 200 mm (height × diameter) latex membrane.
- 10 mm diameter miniature CPT and CPTu cones.

Two apparatuses, a miniature CPT and miniature CPTu cone, were used for testing. The CPT cone provided only a measurement of tip resistance, while the CPTu cone included a friction sleeve and pore pressure transducer. Specifications of the CPT and CPTu apparatuses are provided in Table 1. The 30 MPa CPTu cone was limited to low stress tests ($p' \leq 250$ kPa) due to the tip loadcell capacity. The 100 MPa CPT cone was used for high stress tests ($p' = 1{,}000$ kPa). The 30 MPa CPTu cone was used for low stress tests due to the greater accuracy of the tip resistance load cell. The pore pressure (u_2) measurement also allowed estimation of drainage conditions at the penetration rate used.

Table 1. Miniature CPTu and CPT apparatus specifications

Parameter	CPTu	CPT
Tip resistance: q_t (MPa)	30	100
Frictional resistance: f_s (kPa)	1,000	N/A
Pore pressure: u_2 (kPa)	1,000	N/A

Images of the miniature calibration chamber are provided in Fig. 1 and Fig. 2. A photograph of the 30 MPa CPTu cone and 100 MPa CPT cone is provided in Fig. 3. The miniature cones have an apex angle of 60° and are dimensionally consistent with the full-scale cones.

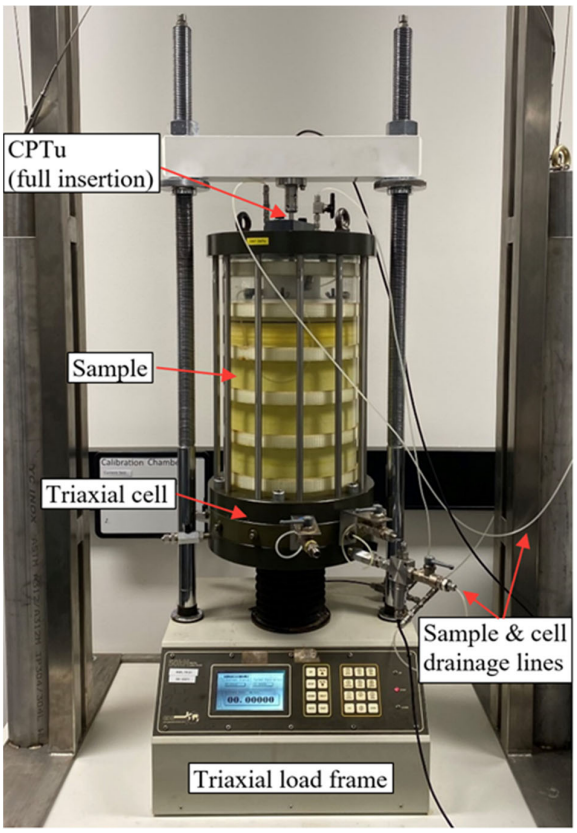

Figure 1. Miniature calibration chamber photograph.

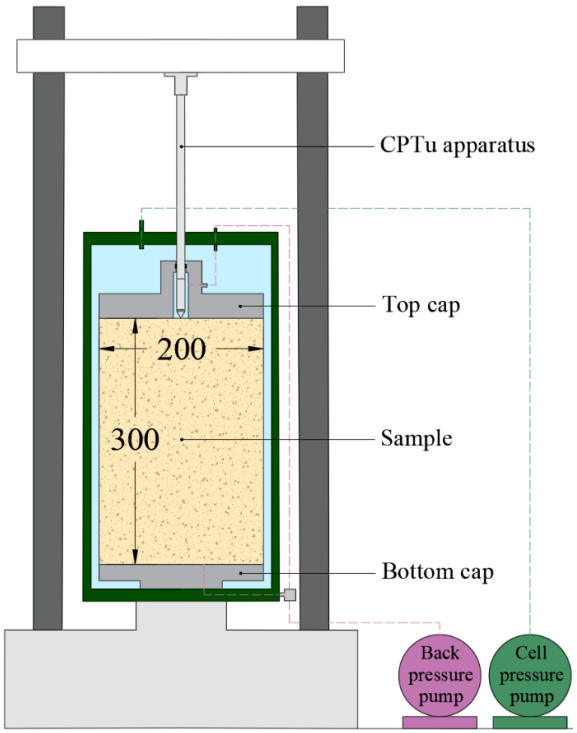

Figure 2. Miniature calibration chamber schematic.

Figure 3. Miniature CPTu (left) and CPT (right) cones.

2.2. Sample preparation

Samples were prepared to a diameter of 200 mm and height of 300 mm. The geometry of the samples allows for a 20:1 ratio of the sample and cone diameter as suggested by various studies (Bolton et al. 1999; Gamez and Olson 2022; Gui et al. 1998; Pournaghiazar, Russell, and Khalili 2012). The sample height of 300 mm allows for penetration of the middle 100 mm at a distance from the top and bottom boundaries which is greater than the distance from the horizontal boundaries.

Samples were prepared to a range of initial densities to test a range of Ψ. Dry pluviation (DP) was used to prepare dense samples but could not be used to prepare loose initial densities. Therefore, moist tamping (MT) was used to prepare samples to loose initial densities. MT samples were observed to be less uniform than DP samples based on variation in tip resistance in the calibration chamber tests. This is consistent with assessments of MT samples by Frost and Park (2003) using optical and x-ray images.

The Ladd (1978) undercompaction method was used to prepare samples by MT. Samples were prepared in 8 layers using an undercompaction ratio of 7%. MT with 10 layers and 3% undercompaction ratio was also tested to try to improve sample uniformity. A range of initial void ratios were targeted for the MT samples by varying the total mass of each layer. DP samples were poured in a continuous layer using a funnel at a constant height above the sample. To achieve a range of initial void ratios, vibration was used with some of the DP samples.

2.3. Test procedure

Tests were performed in a saturated or unsaturated state using two methods. Sands are commonly tested in calibration chamber studies using a combination of saturated and unsaturated states (Jefferies and Been 2015). This is not anticipated to affect the results as negligible suction effects develop in dry sands with low fines content. The fines content of the sand tested was below 5% and the gravimetric water content (GWC) of the DP specimens was approximately zero. The test procedures for saturated and unsaturated tests are provided in Sections 2.3.1 and 2.3.2.

2.3.1. Saturated test procedure

A test procedure was developed based on the method used by Ayala, Fourie, and Reid (2020). To estimate the change in void ratio (e) of the sample during saturation and consolidation, a modified version of the cell calibration technique was adopted. End of test freezing was not used, owing to difficulties in freezing calibration chamber samples due to the sample size and cap arrangement. All tests using this procedure were back pressure saturated to 550 kPa.

The method used by Ayala, Fourie, and Reid was further modified by applying a suction to the sample following penetration by the cone (Steps 11 to 13). This allows the sample to maintain its shape so it can be measured at the end of the test, which allows for estimation of the void ratio based on both the start and end of test measurements. The test procedure is provided below:

1. Prepare a sample using MT or DP to the target density within a split mould. The sample is sealed by the top and bottom caps and latex membrane. During this stage, the cone is housed within a recess in the top cap.
2. Apply a suction of −50 kPa to the sample and measure the height and circumference of the sample at various locations.
3. Close the triaxial cell and fill it with water. Valves to the sample are closed to maintain −50 kPa.
4. Open the valves to the sample and apply 0 kPa cell pressure and −50 kPa back pressure until a constant cell and back volume is achieved.
5. Increase the cell and back pressure in three steps:
    a. 0 kPa cell and −20 kPa back pressure
    b. 30 kPa cell and −20 kPa back pressure
    c. 30 kPa cell and 15 kPa back pressure
6. Flush the sample by opening the top drainage line to atmospheric pressure while applying a constant 30 kPa cell pressure and 15 kPa back pressure. After flushing, reconnect the top drainage line to the back pressure pump and reduce back pressure to 10 kPa.
7. Increase the cell and back pressure in 30 kPa increments, maintaining a maximum effective stress of 50 kPa. Achieve a constant cell and back pressure for each stage before going to the next stage. Repeat this process until reaching cell and back pressure values of 600 and 550 kPa, respectively.
8. Determine the B-value by increasing the cell pressure with valves to the top and bottom drainage lines closed.

9. Consolidate the sample to the target effective stress by increasing the cell pressure in steps with a load increment of 1.
10. Test stage: Insert the cone 240 mm into the sample at a constant rate ≤ 1 mm/s while maintaining a constant cell and back pressure.
11. Further consolidate the sample by applying −50 kPa back pressure while maintaining the cell at a constant pressure from stage 10.
12. Close the valves to the sample, reduce the cell pressure to 0 kPa, and open the cell.
13. Remeasure the sample dimensions as per Step 2.

2.3.2. Unsaturated test procedure

Unsaturated tests were performed under −50 kPa suction using a vacuum pump connected to the back pressure lines. Steps 1 and 2 are the same as for the saturated test procedure in Section 2.3.1 followed by penetration as per Step 10.

This method was used as it reduces the test time; however, only DP samples could be tested as partially saturated MT samples cannot be tested using suction with air or water, for reasons previously described.

2.4. Material properties

Silica fine sand (SFS) was used in the calibration chamber testing. SFS was chosen as it is a reference material that has been extensively tested by the University of Western Australia (UWA) (Fanni, Reid, and Fourie 2022). The material properties are listed in Table 2. The CSL of the SFS was estimated based on 15 CID triaxial tests ranging from 25 to 1,900 kPa consolidation stress. The semi-logarithmic and power law CSL parameters are provided in Table 2 and Fig. 4. Small strain shear modulus (G_{max}) and I_r were estimated from bender element (BE) testing from 20 to 2,800 kPa. These results are presented in Fig. 5.

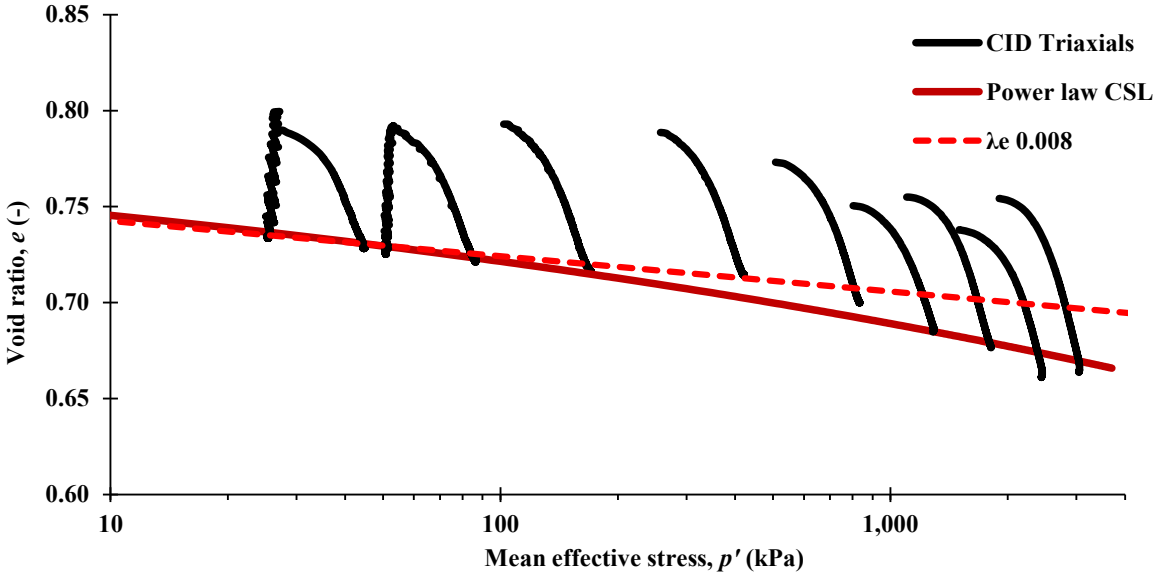

Figure 4. SFS CSL.

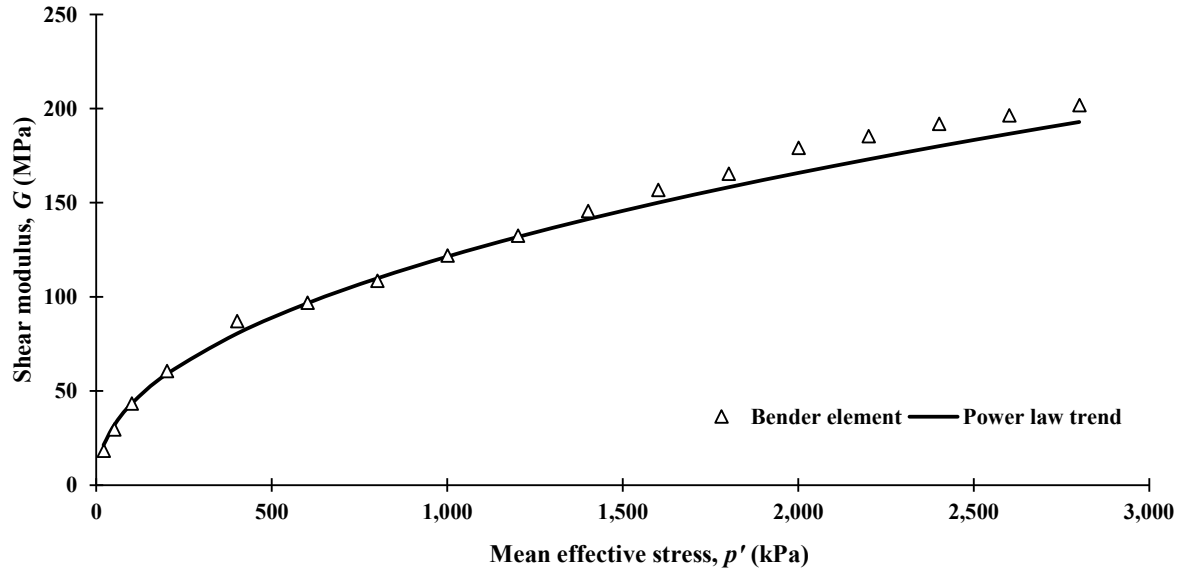

Figure 5. Shear modulus from BE test with trendline fit presented.

Table 2. SFS material properties

Property	Value
Specific gravity: G_s (-)	2.64
Coefficient of uniformity: C_u (-)	1.67
D_{50} (mm)	0.18
CSL: M_{tc}	1.24
CSL logarithmic: Γ (1 kPa)	0.761
CSL logarithmic: λ_e	0.008
CSL power law: A	0.81
CSL power law: B	0.09
CSL power law: C	0.13

3. Calibration chamber tests

13 calibration chamber tests were performed. Low stress tests were performed with saturated and unsaturated conditions at p' = 50 kPa. High stress tests were performed saturated at p' = 1,000 kPa. A single test, CC10, was performed at p' = 250 kPa. The 100 MPa CPT cone was used for the high stress tests due to the limited capacity of the 30 MPa CPTu cone, which was used for the other tests. The test conditions are listed in Table 4.

Typical CPTu equations were used to normalize Q_p (refer Eq. (3)) to be consistent with the CPTwidget output. No excess pore-pressure was measured when using the 30 MPa CPTu cone, so B_q = 0 was applied to tests using the 100 MPa CPT cone. No chamber diameter corrections were applied to the results due to the considerations of sample and CPT cone geometry provided in Section 2.2. Only the data from the middle 100 mm of sample height was used in the interpretation due to proximity to the top and bottom boundaries at 0 to 100 mm and 200 to 300 mm depths (refer Section 2.2).

4. Cavity expansion

CPTwidget Version 2.5, a spherical cavity expansion model using the NorSand constitutive model (Jefferies 1993), was developed by Shuttle (2019). Simulations were run for a range of Ψ between −0.25 to 0.05. Inputs to the model are listed in Table 2 and Table 3. Values for Γ, λ, and M_{tc} were estimated based on the CSL (Fig. 4 and Table 2). The value of χ was estimated based on dense drained triaxial tests calibrated by Reid, Fanni, and Fourie (2023). N was adopted from Fanni, Reid, and Fourie (2022). A typical value for ν for NorSand calibration was adopted. Inputs for H were selected to fit the low stress CPTwidget result to the results of the low stress calibration chamber tests.

Table 3. CPTwidget parameters

Property (unit)	Value
State dilatancy: χ (-)	3.1
Volumetric coupling parameter: N (-)	0.25
Plastic hardening: H (-)	$170–150\Psi$
Elasticity: G_{max} (MPa)	$43(p'/p_{atm})^{0.4}$
Poisson's ratio: ν (-)	0.2

Values for G were adopted based on BE testing, described in Section 2.4, which were also used to select the inputs for I_r. The following simulations were run for low and high stress:

- Low stress:
  - p' = 50 kPa
  - I_r = 580
- High stress:
  - p' = 1,000 kPa
  - I_r = 120

An additional simulation was run at high stress with inputs (Γ = 0.8 and λ_e = 0.016) which were fit to the tangent of the CSL at 1,000 kPa. This was simulated to estimate the effect of curvature on the CPTwidget results.

5. Results

The results of the calibration chamber tests are listed in Table 4. Figure 6 illustrates the results and the trendline fit to the low stress data using Eq. (3). Tip resistance presented is the mean from the middle 100 mm of the sample. Error bars on the y-axis indicate the variability of tip resistance within the middle 100 mm of the sample.

The outputs of the CPTwidget simulation at low stress and high stress are plotted in Fig. 7. The high stress simulation with Γ and λ_e tangential to the CSL at 1,000 kPa is also included.

Table 4. Calibration chamber test results

Test	Effective stress, p' (kPa)	Sample preparation	Saturation	Void ratio,[a] e (-)	State parameter,[a] Ψ (-)	Mean normalised tip resistance, $Q(1-B_q)+1$ (-)
1	50	DP	Unsaturated	0.68	−0.08	52.5
2	50	DP	Unsaturated	0.67	−0.08	63.2
3	50	DP	Unsaturated	0.60	−0.15	148.8
4	50	DP	Unsaturated	0.62	−0.14	113.7
5	50	DP	Unsaturated	0.65	−0.10	83.3
6	50	DP	Unsaturated	0.68	−0.07	61.3
7	50	DP	Unsaturated	0.53	−0.23	176.9
8	50	MT	Saturated	0.74	−0.01	70.9
9	50	MT	Saturated	0.60	−0.15	177.9
10	250	MT	Saturated	0.79	0.04	43.4
11	1,000	DP	Saturated	0.71	0.02	30.7
12	1,000	DP	Saturated	0.62	−0.06	83.2
13	1,000	DP	Saturated	0.68	−0.01	60.0

Note: a) Estimated after back pressure saturation and consolidation, but before penetration.

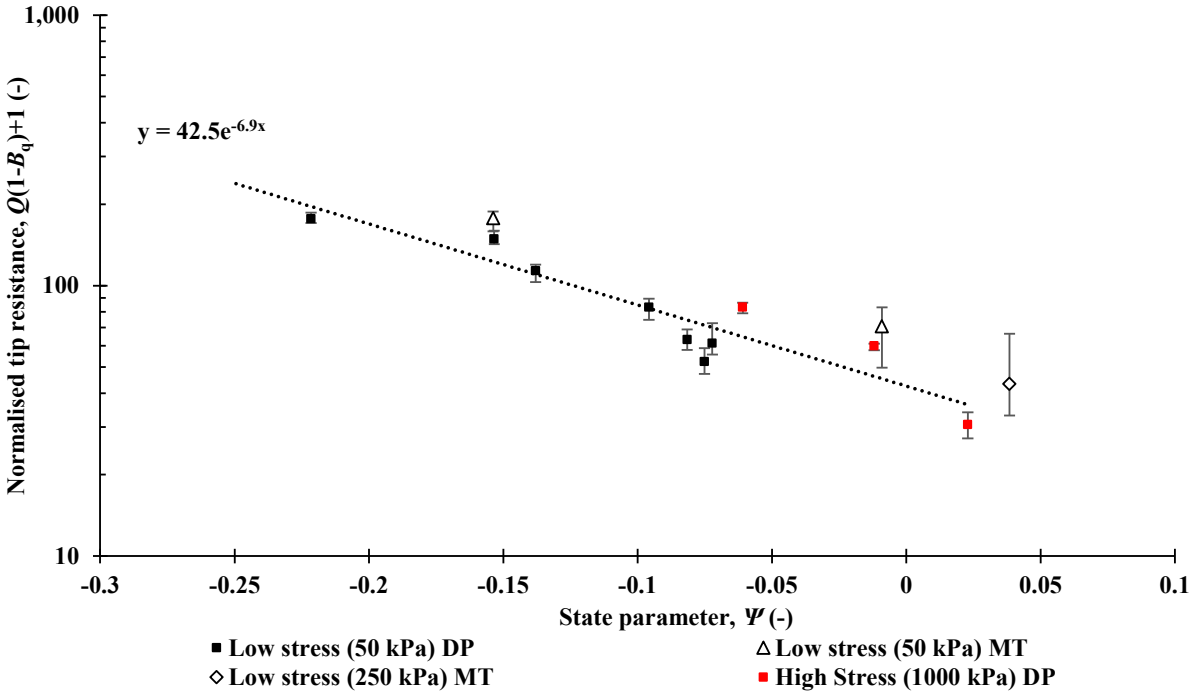

Figure 6. Results of calibration chamber tests at low and high stress.

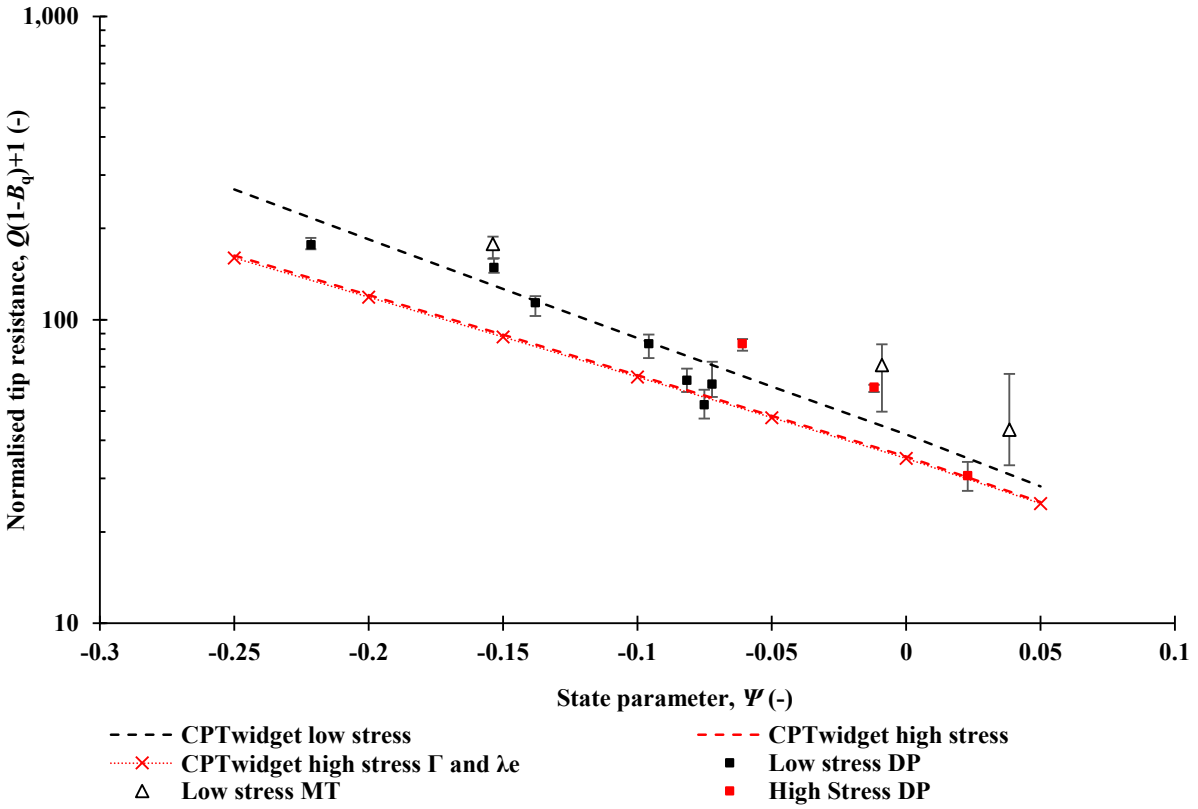

Figure 7. CPTwidget simulations at low and high stress compared to calibration chamber tests.

6. Discussion

The calibration of SFS at low stress showed a linear semi-logarithmic trend consistent with the form of Eq. (3). Based on the findings of Salgado, Mitchell, and Jamiolkowski (1998) and Been et al. (1986), it is anticipated that the influence of boundary conditions would result in a reduction of $Q(1-B_q)+1$ at low Ψ. No significant reduction has been observed in the data. Future testing on larger diameter samples of SFS should be undertaken to understand the effect of boundary conditions.

DP tests resulted in less variability of tip resistance within the middle 100 mm of penetration depth, compared to MT tests. Saturated tests (low stress MT and high stress DP) showed a generally higher trend than the unsaturated tests. Further tests are required to confirm this trend.

Comparing the results of the high and low stress calibration chamber tests indicates that the high stress tests tend towards the same trendline as the low stress tests. Denser tests could not be performed at p' = 1,000 kPa due to the 100 MPa capacity of the CPT cone. A higher capacity CPT cone will be obtained to allow testing at lower Ψ and high stresses.

The result of the CPTwidget simulation indicated a lower and flatter trend (lower k and m) at high stress compared to low stress. Additionally, the high stress CPTwidget simulation was noticeably curved compared to the low stress simulation on the semi-logarithmic plot.

The CPTwidget tip resistance result at high stress was 11% to 40% lower than the simulation results at low stress over the modelled range of Ψ. This difference is less pronounced than for Ticino sand (Jefferies and Been 2015) which demonstrated a reduction of 54% to 75% between p' of 27 and 451 kPa. The I_r range of the Ticino sand was approximately 65 to 650 which is larger than for SFS (refer Section 4) even though the range of p' was much less.

The high stress CPTwidget output is at the lower bound of the calibration chamber data and does not fit well with 2/3 of the high stress tests. However, as the scatter in the calibration chamber data is of a similar magnitude to the difference in CPTwidget results between low and high stress, a clear trend cannot be identified. Similar scatter is shown in the Jefferies and Been (2015) calibration chamber database. The scatter is generally attributed to variability within samples and difficulty estimating void ratio in large samples. Further work is required to identify a more consistent trend and confirm the trendline for high stress tests.

The CPTwidget parameters were calibrated to fit the low stress simulations with the low stress calibration chamber data. Therefore, neither the results of the low stress or high stress simulation can be determined to provide a better fit to the data. However, the effect of stress, and subsequent change in I_r, is more significant in CPTwidget than observed in the calibration chamber data.

Future work is planned on sand with significant curvature of the CSL to better understand the effect of changing I_r and λ at high stress. Additional work should be undertaken on materials under undrained penetration to understand if similar behavior is observed.

Acknowledgements

The authors are grateful for the ongoing support of WSP Australia which provided financial support for the research and calibration chamber equipment. Additionally, we acknowledge the contributions of personnel in the WSP Perth Laboratory and the University of Western Australia.

References

Ayala, J., A. Fourie, and D. Reid. 2020. "Cone penetration testing on silty tailings using a new small calibration chamber." *Géotechnique Letters* 10, no. 4: 492–497. https://doi.org/10.1680/jgele.20.00037

Been, K., J. H. A. Crooks, D. E. Becker, and M. G. Jefferies. 1986. "The cone penetration test in sands, part 1: state parameter interpretation." *Géotechnique* 36, no. 2: 239–249. https://doi.org/10.1680/geot.1986.36.2.239

Been, K., J. H. A. Crooks, and M. G. Jefferies. 1988. "Interpretation of material state from the CPT in sands and clays." In *Penetration testing in the UK*, edited by the Institution of Civil Engineers, 215–218. London: Thomas Telford. https://www.icevirtuallibrary.com/doi/abs/10.1680/ptituk.13773.0034

Been, K., and M. G. Jefferies. 1992. "Towards systematic CPT interpretation." In *Predictive soil mechanics: Proceedings of the Wroth Memorial Symposium*, 121–134. London: Thomas Telford. https://www.icevirtuallibrary.com/doi/abs/10.1680/psm.19164.0008

Bolton, M. D., M. W. Gui, J. Garnier, J. F. Corte, G. Bagge, J. Laue, and R. Renzi. 1999. "Centrifuge cone penetration tests in sand." *Géotechnique* 49, no. 4: 543–552. https://doi.org/10.1680/geot.1999.49.4.543

Damavandi-Monfared, S., and A. Sadrekarimi. 2015. "Development of a miniature cone penetrometer for calibration chamber testing." *Geotechnical Testing Journal* 38, no. 6: 878–892. https://doi.org/10.1520/GTJ20150036

Fanni, R., D. Reid, and A. Fourie. 2022. "Effect of principal stress direction on the instability of sand under the constant shear drained stress path." *Géotechnique*, ahead of print: 1–17. https://doi.org/10.1680/jgeot.22.00062

Frost, J. D., and J. Y. Park. 2003. "A critical assessment of the moist tamping technique." *Geotechnical Testing Journal* 26, no. 1: 57–70. https://doi.org/10.1520/GTJ11108J

Gamez, J. A., and S. M. Olson. 2022. "Compressibility-based interpretation of cone penetrometer calibration chamber tests and corresponding boundary effects." *Geotechnical Testing Journal* 45, no. 4: 778–796. https://doi.org/10.1520/GTJ20210129

Gui, M. W., M. D. Bolton, J. Garnier, J. F. Corte, G. Bagge, J. Laue, and R. Renzi. 1998. "Guidelines for cone penetration tests in sand." In *Proceedings of the International Conference Centrifuge 98, Tokyo, Japan, 23–25 September 1998,* vol. 1, edited by T. Kimura, O. Kusakabe, and J. Takemura, 155–160. Rotterdam: A. A. Balkema. http://www-civ.eng.cam.ac.uk/geotech_new/people/bolton/mdb_pub/69_centrifuge98_155_160.PDF

Jefferies, M. G. 1993. "NorSand: a simple critical state model for sand." *Géotechnique* 43, no. 1: 91–103. https://doi.org/10.1680/geot.1993.43.1.91

Jefferies, M. G., and K. Been. 2015. *Soil liquefaction: a critical state approach*, 2nd ed. Boca Raton, FL: CRC Press. https://doi.org/10.1201/b19114

Ladd, R. S. 1978. "Preparing test specimens using undercompaction." *Geotechnical Testing Journal* 1, no. 1: 16–23. https://doi.org/10.1520/GTJ10364J

Pournaghiazar, M., A. R. Russell, and N. Khalili. 2012. "Linking cone penetration resistances measured in calibration chambers and the field." *Géotechnique Letters* 2, no. 2: 29–35. https://doi.org/10.1680/geolett.11.00040

Reid, D., R. Fanni., and A. Fourie. 2023. "Is the maximum shear stress, in an assumed constant shear drained stress path, really constant?" In *10th European Conference on Numerical Methods in Geotechnical Engineering (NUMGE2023)*, edited by L. Zdravkovic, S. Kontoe, D. M. G. Taborda, and A. Tsiampousi, 1–6. https://doi.org/10.53243/NUMGE2023-227

Shuttle, D. A. 2019. "CPTwidget: a finite element program for soil-specific calibration of the CPT."

Shuttle, D. A., and J. Cunning. 2007. "Liquefaction potential of silts from CPTu." *Canadian Geotechnical Journal* 44, no. 1: 1–19. https://doi.org/10.1139/t06-086

Shuttle, D. A., and M. G. Jefferies. 2016. "Determining silt state from CPTu." *Geotechnical Research* 3, no. 3: 90–118. https://doi.org/10.1680/jgere.16.00008

Salgado, R., J. K. Mitchell, and M. Jamiolkowski. 1998. "Calibration chamber size effects on penetration resistance in sand." *Journal of Geotechnical and Geoenvironmental Engineering* 124, no. 9: 878–888. https://doi.org/10.1061/(ASCE)1090-0241(1998)124:9(878)